Effect of Filling Pressure on Post-Arc Gap Recovery of N_2

Fahim Abid, Kaveh Niayesh and **Egil Viken**
Norwegian University of Science and Technology (NTNU)
Department of Electric Power Engineering
Trondheim, Norway

Nina Sasaki Støa-Aanensen, Erik Jonsson and **Hans Kristian Meyer**
SINTEF Energy Research
Trondheim, Norway

ABSTRACT

Experimental investigation of the effect of filling pressure on the post-arc dielectric recovery characteristics of nitrogen is reported in this paper. A half-cycle arc current duration of 540 µs followed by a 10 kV pulse with a rise rate of 150 V/µs is applied across the contact gap. The pulse is applied from 10 µs to 10 ms after the current zero. First, a free-burning arc is studied without any forced gas flow. The effect of the gap distance on the recovery process is studied by using two different inter-electrode gaps: 20 mm and 50 mm. The effect of arc current on the recovery process is investigated by using current amplitudes of 275 A and 425 A. Moreover, the effect of forced nitrogen flow near current zero is explored using two different arrangements: self-blast and puffer type. Four different nitrogen filling pressures are studied: 1, 20, 40, and 80 bar, the latter two being in the supercritical region. The experimental results show that, in the free-burning arc configuration, the breakdown voltage of the contact gap increases faster with the increase of the filling pressure. A gap of 50 mm recovers quicker than a 20 mm gap, whereas no strong current dependency is observed on the recovery characteristics in the investigated range. In the free-burning arc configuration, just after the current zero up to approximately 300 µs, the breakdown voltage at high filling pressure is found to be lower than at 1 bar. Forced gas flow, however, significantly enhances the dielectric recovery at a high filling pressure, also in the thermal phase.

Index Terms — **supercritical fluid, arc discharge, dielectric recovery, ultrahigh-pressure arc, switchgear**

1 INTRODUCTION

THE need to transfer power to and from offshore installations (wind farms and offshore mining) will lead to the development of offshore substations. To materialize such a substation, there are two possible paths to follow: one path is to place the electrical equipment on a platform or floater above sea level. Another path is to directly place the equipment on the seafloor and control it remotely. Among these two options, the latter is more economically viable [1]. The conventional solution is to place the power equipment (i.e., circuit breaker of vacuum or gas technology) inside a pressure-proof vessel [2]. Medium voltage gas circuit breakers are generally filled up to 1.3 bar filling pressure and sealed at the manufacturer site [3]. To transfer and control electrical power from the high-pressure water environment at seabed into the pressure-proof vessel, various feedthroughs and penetrators are required. All these arrangements used to cope with the high-pressure water environment, add considerable technical complexity and cost. A novel concept is developed, where the interruption chamber can be filled with high-pressure gas to reduce the differential pressure exerted on the encapsulation. Reducing the differential pressure will substantially reduce the cost and complexity of the encapsulations and feed-throughs.

If the pressure and temperature of a gas exceed a critical point, it enters the supercritical (SC) region [4]. In this SC region, liquid and gas states are united and indistinguishable. For example, an SC fluid has a high density, while the viscosity is low like a gas. The properties of an SC fluid are believed to be in favor of a successful current interruption medium [5]. In this paper nitrogen (N_2) is chosen for its low critical pressure (33.5 bar) [6]. Moreover, N_2 is abundant in air and hence, environmentally benign.

In order to successfully interrupt the current, the breakdown voltage of the contact gap must be higher than the transient recovery voltage at any time after the current zero (CZ) [7]. Many investigations are focused on the dielectric recovery of

Manuscript received on 8 February 2020, in final form xx Month 20yy, accepted xx Month 20yy. Corresponding author: F.Abid.

This is the author accepted version of an article published in IEEE transactions on dielectrics and electrical insulation
http://dx.doi.org/10.1109/TDEI.2020.008844

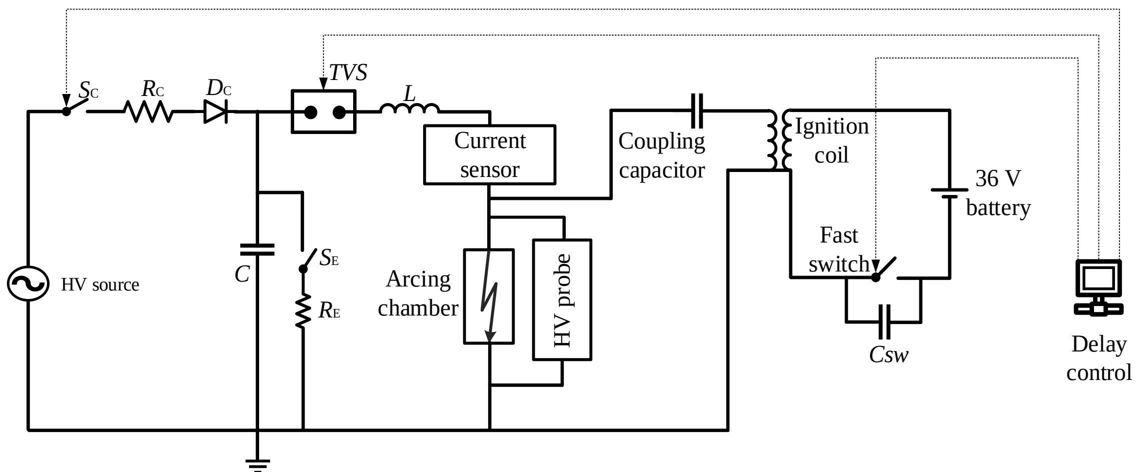

Figure 1. Schematics of the test circuit. An ignition coil is used to generate a 10-kV high voltage pulse which is applied at different instants after CZ.

the post-arc channel at 1 bar or slightly higher pressure arcs typical of land-based circuit breakers; e.g. [8]–[11]. In contrast, arc characteristics at an extremely high gas pressure including the SC region are not a well-explored area. Recently, a series of experiments have been conducted to study the arc properties at extremely high N_2 filling pressure in the SC region. First, a free-burning arc and the influence of tube constriction on the arc have been investigated in the SC state and beyond, up to 80 bar filling pressure during the high current phase [12], [13]. Some further investigations were focused on the region near CZ, where the effect of N_2 filling pressure on the thermal interruption performance is evaluated [14]–[16]. The arc voltage is reported to increase with the filling pressure, whereas no abrupt change in arc voltage is observed during the transition of N_2 from gas to SC region [12]. As a result, the energy deposition in the arc channel increases at a higher filling pressure. The calculated arc diameter reduces with increasing pressure [13].

In this paper, the pressure dependence of the dielectric recovery characteristics of N_2 arcs is investigated including the SC region. To evaluate the dielectric recovery of the contact gap, a 10 kV high voltage (HV) pulse (rise time of approximately 70 µs) is applied between the electrodes at different instants after CZ. The time of the pulse is varied from 10 µs and 10 ms after CZ. The free-burning arc is studied at 1 (atmospheric pressure), 20, 40, and 80 bars, the latter two being in the SC region. Some of these results are reported in a conference paper [17]. In the free-burning arrangement, the effect of the contact gap and the current amplitude on the recovery characteristics is also studied at different filling pressures. In order to efficiently cool the arc near CZ and interrupt the current, the arc in a gas circuit breaker is generally subjected to a forced gas flow [7]. In commercial gas circuit breakers, two of the most commonly used techniques to cool the arc are self-blast and puffer type [7]. In this paper, two different mechanisms (self-blast and puffer arrangement) are adopted to evaluate the effect of forced gas flow on the post-arc dielectric recovery of N_2 at extremely high filling pressures. The breakdown voltages at different instants after CZ are used to analyze the recovery characteristics.

2 EXPERIMENTAL SETUP

The schematics of the test circuit and measurement system used in this study are shown in Figure 1. The high voltage (HV) energy storing capacitor, C is first charged to a preset value. It is then discharged by the triggered vacuum switch (TVS) through the inductor, L and further through the ignition copper wire inside the arcing chamber. The arcing chamber is a 15.7 liters, 500 bar rated pressure tank. The photo of the test setup and the corresponding value of the circuit parameters are shown in Figure 2 and Table 1 respectively. Once the TVS is closed, the current starts to flow, and the arc is initiated by the melting of the thin copper wire. The content of the copper in the atmospheric arcs at least seems to be in the range of 1-2% and therefore, the influence of metal vapor is not significant [18]. Furthermore, to reduce the effect of metal vapor between the different tests, all the tests are conducted using a 40 µm copper ignition wire. The current flow through the arc until the first CZ crossing, where the current is interrupted by the TVS. The right part of the test circuit in Figure 1 is a voltage pulse generator circuit using an ignition coil. An HV pulse of 10 kV (rise rate of 150 V/µs) is applied between the electrodes at different times after CZ. A coupling capacitor is placed between the ignition coil and the arcing chamber. The

Figure 2. Photos of the lab setup. (a) HV source. (b) Capacitor, C. (c) Inductor, L. (d) Arcing chamber. (e) N_2 cylinder.

This is the author accepted version of an article published in IEEE transactions on dielectrics and electrical insulation
http://dx.doi.org/10.1109/TDEI.2020.008844

Table 1. Test circuit parameters and their values.

Circuit Parameters	Value
HV Source	220V: 40 kV Transformer
Capacitor, *C*	4.8 µF
Inductor, *L*	6 mH
Coupling Capacitor	500 pF

coupling capacitor blocks the arc current to flow through the ignition coil while allowing the HV pulse to be applied across the electrodes. After applying the HV pulse, either the electrode gap withstands the applied voltage, or a breakdown occurs.

As the arc voltage increases with the filling pressure, for a given predefined charging voltage, the arc current amplitude varies with the filling pressure. While the arc current amplitude is 425 A at 1 bar, it is limited to 400 A at 80 bar filling pressure by the same charging voltage of the capacitor, *C*. One possible solution to overcome slightly different arc currents would be to increase the charging voltage of the capacitor. However, changing the charging voltage would also influence the stored energy of the capacitor. Hence, in this paper, the charging voltage of the capacitor is kept constant while the slight change of the arc current amplitude is considered as the property for arc burning at different filling pressures. The CZ crossing also changes by a few microseconds when the arc voltage varies. The timing of the application of HV pulse is compensated for different filling pressures to get the desired time to pulse after CZ.

Two HV probes with different voltage ranges are used to measure the HV pulse and the arc voltage. The arc current is measured by a shunt resistor. Both the HV probes and the current sensor are connected outside of the pressure tank and on the HV side of the arcing chamber. For the puffer arrangement, the movement of the piston is recorded by a linear displacement sensor while the blow pressure is recorded by a dynamic pressure sensor mounted at the throat of the puffer.

2.1 TEST OBJECTS

Three different test arrangements are used in this paper. The main bulk of the tests are conducted with a simple pin and ring electrode pair, resulting in a free-burning arc configuration, see Figure 3a. In the free-burning arrangement, the arc burns freely without any forced gas flow. At 50 mm inter-electrode gap and with a current of 425 A, the pressure dependence of the recovery characteristics is studied at four different filling pressures: 1, 20, 40, and 80 bar, as can be seen in Table 2. Then the inter-electrode gap is changed to 20 mm to study the distance dependency of the recovery process. For the 20 mm gap distance, three different filling pressures are investigated: 1, 20, and 40 bar. Finally, the current amplitude is varied to 275 A to investigate the current dependency of the dielectric recovery in the contact gap. For the current dependency, two different filling pressures are tested: 1 and 40 bar.

To study the effect of forced gas flow on the recovery process, two different arrangements are studied. A simple self-blast arrangement is adopted where the arc burns inside a PTFE tube with vents in the middle, see Figure 3b. Two opposite holes of 3 mm diameter in the middle of the inter-electrode gap act as the vents. The pin electrode is pushed inside the PTFE tube in such a way that it blocks the gas flow out through the pin electrode. A heating volume of 3.17 cm^3 is attached to the ring electrode. During the high current phase, a part of the ablated PTFE vapor directly leaves through the vent, while the rest is stored in the heating volume. As a result, the pressure in the heating volume increases. The high pressure in the heating volume forces a relatively cold gas flow through the vent of the tube and cools the arc near the CZ. For the self-blast arrangement, two different filling pressures are tested: 1 and 40 bar, see Table 2. The reference measurement in the self-blast arrangement is conducted without the heating volume, i.e., the arc burns inside the PTFE tube only without any backflow of gas near CZ. After every 10 experiments, the PTFE tube is changed, and a new tube is mounted.

Table 2. Inter-electrode gap, corresponding arc current and the tested filling pressure for different test arrangements.

Test object	Inter-electrode gap [mm]	Arc current [A]	Filling pressure tested [bar]
Free-burning	50	425	1, 20, 40, 80
Free-burning	20	425	1, 20, 40
Free-burning	50	275	1, 40
Self-blast	50	425	1, 40
Puffer	20	425	1, 20, 40

The last test arrangement is a puffer-type configuration as shown schematically in Figure 3c. The puffer mechanism works by pre-charging a spring which is kept in position by an electromagnet. A 10 mm long PTFE nozzle with an inner diameter of 4 mm is mounted with the ring electrode. The total

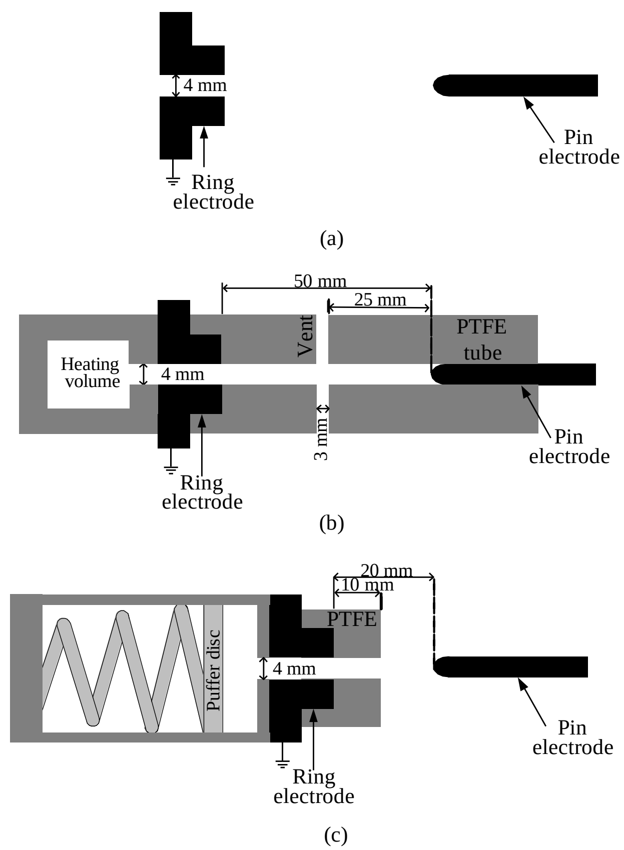

Figure 3. Test arrangement. (a) Free-burning arc, (b) self-blast arrangement, (c) puffer arrangement.

This is the author accepted version of an article published in IEEE transactions on dielectrics and electrical insulation
http://dx.doi.org/10.1109/TDEI.2020.008844

inter-electrode gap in the puffer setup is kept fixed at 20 mm. As the filling pressure increases, the density and the viscosity increase too. As a result, for the same pre-charging of the spring, the travel curve of the piston varies at different filling pressures. In this paper, the spring is released at instants that result in a similar upstream pressure difference at CZ for all filling pressures. To study the effect of forced gas flow on the same electrode and nozzle arrangement, reference measurements were also conducted. The reference measurement in the puffer arrangement is conducted without pre-charging the spring, i.e., the arc burns partly inside the PTFE nozzle and partly outside the nozzle without any forced gas flow.

2.2 PROCEDURE

All the experiments are conducted in a fixed electrode arrangement and the arc is initiated by the melting of a thin copper wire of 40 µm diameter. The ignition copper wire is mounted on the electrode by hand and then the flange of the pressure tank is closed. The pressure tank is first flushed and then filled with industrial-grade N_2 to ensure 99% N_2 inside the pressure tank. The energy storing capacitor, *C*, is charged to a predefined charging voltage of 15 kV to generate the arc current of 425 A. For the 275 A current settings, the charging voltage is reduced to 10 kV. Once *C* is charged to the predefined level, a computer program controls the timing of the switches S_C, TVS, HV pulse and release of the electromagnet (for the puffer arrangement). To investigate the breakdown or the hold voltage at different instants after CZ, the timing of the HV pulse is varied. After each test, the over-pressure in the pressure tank is released, and the ignition copper wire is mounted by hand. A total of 175 tests were conducted in this work.

3 EXPERIMENTAL RESULTS

A typical measurement of the arc current, the voltage across the contact gap at 20 bar pressure are shown in Figure 4. The arc is established by the melting of the copper wire (marked as the voltage peak at 0.5 ms before CZ). Once the arc is formed, the arc current continues to flow until CZ, where the current is interrupted by the TVS. Due to the application of the voltage pulse after CZ between the electrodes, a breakdown may occur

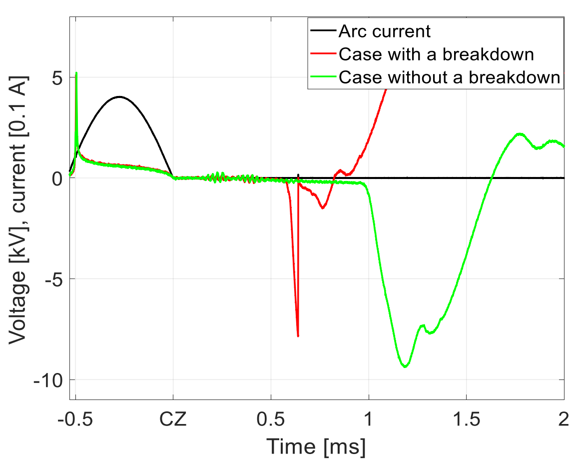

Figure 4. A measurement showing the arc current, a case with a breakdown (red line) and a case without a breakdown (green line).

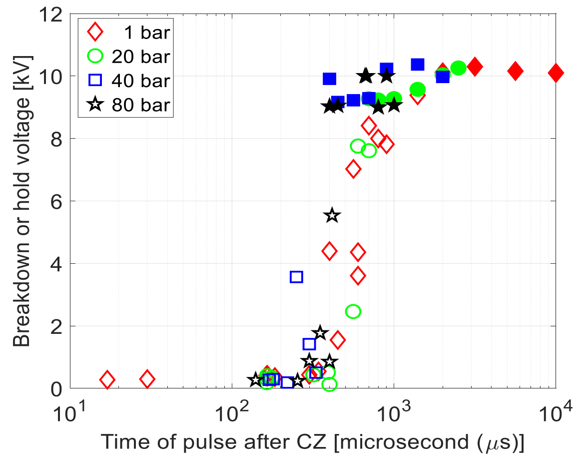

Figure 5. Breakdown or hold voltage at different instants after CZ for 50 mm gap distance at an arc current of 425 A in free-burning arrangement. The filled markers represent withstand voltages whereas the empty markers represent breakdown voltages.

in the hot, conductive channel. If a breakdown occurs, it is marked by a voltage collapse at 7.8 kV, see the red line at approximately 700 µs after CZ in Figure 4. In the case of without a breakdown, the contact gap withstands the applied HV pulse, as can be seen by the green line in Figure 4. For the case without a breakdown, the peak of the voltage pulse is recorded.

Just after CZ, voltage oscillations across the contact gap are recorded due to the stray capacitances, which is independent of the applied HV pulse. The peak of the voltage oscillations is approximately 400 V with a rise rate of approximately 125 V/µs. As the breakdown strength of the contact gap just after CZ is very low, such voltage oscillations may cause breakdowns. The breakdowns generated by these voltage oscillations are also considered to analyze the recovery characteristics.

3.1 FREE-BURNING ARC

Breakdown or hold voltages as a function of time after CZ in the free-burning arrangement for 50 mm gap distance at different pressures are shown in Figure 5. The filled and empty markers represent the hold voltage and the breakdown voltage respectively. At atmospheric pressure (1 bar) the measured breakdown voltages are close to 330 V between 10 µs and 300 µs after CZ for a 50 mm contact gap. The breakdown voltage gradually increases after 300 µs after CZ. At 1 bar pressure, the HV pulse does not generate a breakdown when the pulse is applied later than 2 ms after CZ.

The breakdown voltage between 10 to 300 µs after CZ at a high filling pressure (20, 40, and 80 bar), however, is around 100 V for 50 mm gap distance, see Figure 5. Before 300 µs, the breakdown voltage at a higher filling pressure is lower compared to the measured breakdown voltages at 1 bar filling pressure. After 300 µs, however, the breakdown voltage rises faster as the N_2 filling pressure is increased. The gap withstands the applied HV pulse after 800 µs and 400 µs for N_2 filling pressure of 20 and 40 bar, respectively.

This is the author accepted version of an article published in IEEE transactions on dielectrics and electrical insulation
http://dx.doi.org/10.1109/TDEI.2020.008844

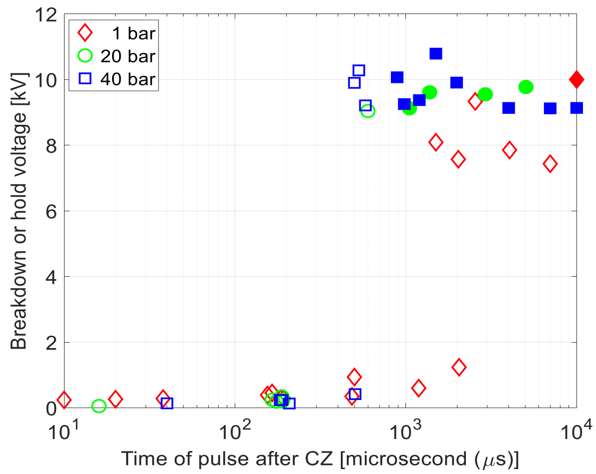

Figure 6. Breakdown or hold voltages at different instants after CZ for 20 mm long inter-electrode gap and an arc current amplitude of 425 A in free-burning arrangement. The filled markers represent withstand voltages whereas the empty markers represent breakdown voltages.

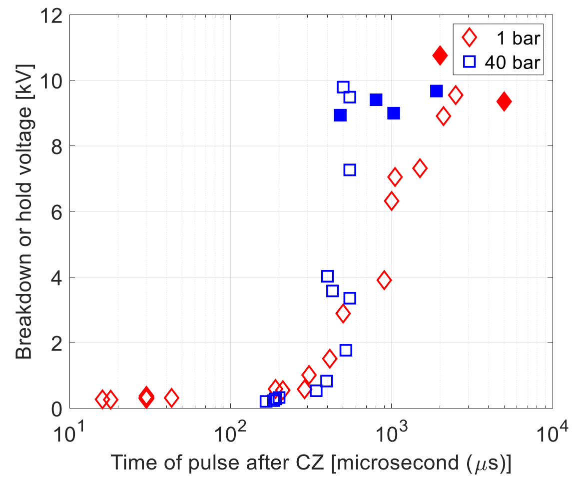

Figure 7. Breakdown or hold voltage at different instants after CZ for 50 mm inter-electrode gap distance for arc current of 275 A in free-burning arrangement. The filled markers represent withstand voltages whereas the empty markers represent breakdown voltages.

3.1.1 INTER-ELECTRODE GAP

The gap dependency of the post-arc recovery process is studied in the free-burning arrangement by conducting the experiments at a 20 mm gap at 1, 20, and 40 bar N_2 filling pressures. The breakdown or hold voltages at different instants after CZ for different filling pressures are plotted in Figure 6. As was observed for the 50 mm case, the 20 mm gap recovers faster at 40 bar than at 1 bar. When compared between different gap distances, the 20 mm gap recovers more slowly than the 50 mm gap for all pressures (see Figure 5 and Figure 6). At 1 bar filling pressure at 50 mm gap, when the HV pulse was applied later than 2 ms after CZ, the gap withstood the voltage. When the inter-electrode gap is reduced to 20 mm, dielectric breakdowns were observed for pulses earlier than 10 ms after CZ. At 40 bar, the corresponding minimum times to hold the applied pulse are 400 μs and 700 μs for 50 mm and 20 mm gap distances, respectively.

3.1.2 ARC CURRENT

The effect of arc current amplitude on the recovery process is studied by carrying out experiments for an arc current amplitude of 275 A. In this case, the gap distance is kept fixed at 50 mm. Two different filling pressures are used: 1 and 40 bar. The breakdown or hold voltage at different instants after CZ is plotted in Figure 7. Similar to what is observed previously, at 275 A arc current a faster increase of the breakdown voltage at 40 bar is observed compared to 1 bar filling pressure. No significant change in recovery time is observed between the two tested current levels (see Figure 5 and Figure 7).

3.2 SELF-BLAST ARRANGEMENT

The breakdown or hold voltage at different instants after CZ for different filling pressures for the self-blast arrangement is shown in Figure 8. The time of HV pulse application after CZ was varied from 20 μs to 500 μs for both N_2 pressures (1 and 40 bar). In contrast to the free-burning arc arrangement, no breakdowns were observed neither at 1 bar nor at 40 bar filling pressures. For the cases without a heating volume, i.e. for the reference measurements, as the time to HV pulse is reduced, the amplitude of the applied pulse went down. Similarly, for the cases with the heating volume, i.e., self-blast type, few cases are observed at 40 bars when the amplitude of the applied pulse is reduced. The reduction of the amplitude of the HV pulse is perhaps linked with the high post-arc conductivity immediately after CZ.

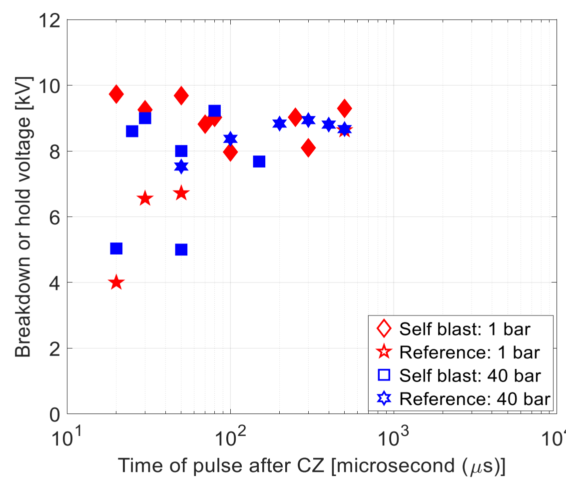

Figure 8. Breakdown or hold voltage at different instants after CZ in self-blast arrangement for 425 A arc current. The filled markers represent withstand voltages whereas the empty markers represent breakdown voltages.

3.3 PUFFER ARRANGEMENT

The viscosity and the density vary with the filling pressure. As a result, for the same spring setting, the travel curve and the subsequent upstream pressure difference vary for different filling pressures. The travel curve and the upstream pressure difference for different filling pressures are plotted in Figure 9. For the full stroke of the piston, it takes approximately 70 ms, 83 ms, and 110 ms at 20, 40, and 80 bar filling pressures, respectively. The arc experiments were conducted at the time when the piston remains roughly in the middle of its stroke and the upstream pressure difference is in the range of 80-90 mbar. The initiation of the arc can be seen by the sharp spike in the

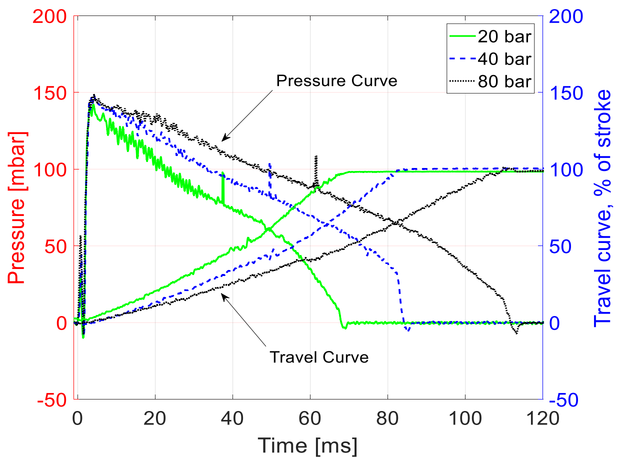

Figure 9. Travel curve and upstream pressure difference of the puffer for different filling pressure.

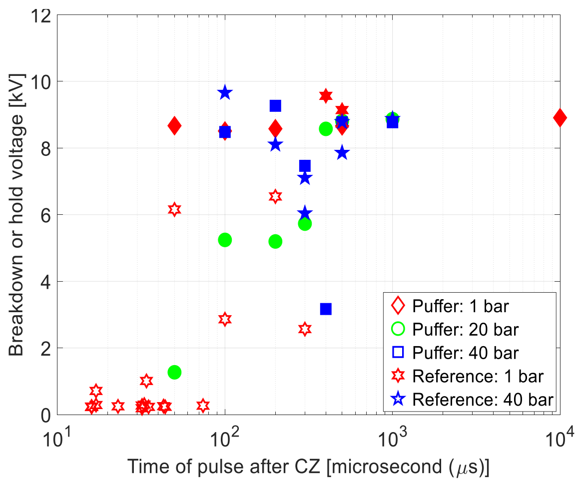

Figure 10. Breakdown or hold voltage at different instants after CZ for puffer arrangement for arc current of 425 A at 950 Hz. The filled markers represent withstand voltages whereas the empty markers represent breakdown voltages.

pressure curve at 38 ms, 50 ms, and 62 ms at 20, 40, and 80 bar respectively, as shown in Figure 9. In this way, a similar upstream pressure difference can be ensured for all the different filling pressures.

The breakdown or the hold voltage at different instants after CZ for puffer arrangements at three different filling pressures are plotted in Figure 10. Reference measurements were conducted without any puffer movement, i.e., the arc burnt in the nozzle without any forced gas flow. No breakdowns were observed without forced gas flow, when the pulse was applied after 400 µs at 1 bar filling pressure. A voltage pulse before 400 µs caused a breakdown for reference measurements at 1 bar. For reference measurement at 40 bar filling pressure, however, no breakdown was observed even for the pulse at 100 µs. For the cases with a forced gas flow, no breakdown was observed at neither of the filling pressures.

The amplitude of the HV pulse is observed to go down as the time of pulse approaches CZ, as shown in Figure 11. This is perhaps due to the higher conductivity of the post-arc channel near CZ. At a high filling pressure (e.g., 20 bar, 40 bar), the damping of the applied HV pulse is greater than at 1 bar pressure. It has been observed that for some cases, the applied 10 kV pulse is limited to 1 kV when the time to pulse is 200 µs or less after CZ for 40 bar or 50 µs for 20 bar filling pressure. As a result, no test was possible to be carried out for a time to pulse of less than 50 µs.

4 DISCUSSION

As the current approaches zero, the arc temperature decreases. However, the temperature change in the arc channel at CZ is not instantaneous. After CZ, when the temperature of the post-arc channel continues to drop below a certain level, the ionized particles start to recombine, which reduces the number of free charge carriers [19], [20]. As a result, the post-arc breakdown voltage of the contact gap depends on the gap temperature. Many factors influence the temperature decay of the gap which includes the geometry of the gap and the physical properties of the medium e.g., thermal conductivity, density, specific heat and viscosity [21].

In the free-burning arrangement, just after CZ until several hundred microseconds, the breakdown voltage is observed to be the same for any particular filling pressure. For 1 bar, the breakdown voltage is approximately 330 V, whereas for the higher filling pressures (e.g., 20 bar, 40 bar, 80 bar) the breakdown voltage just after CZ is approximately 100 V. Just after CZ, a positive ion space charge layer is formed adjacent to the pulse cathode when the voltage stress appears across the

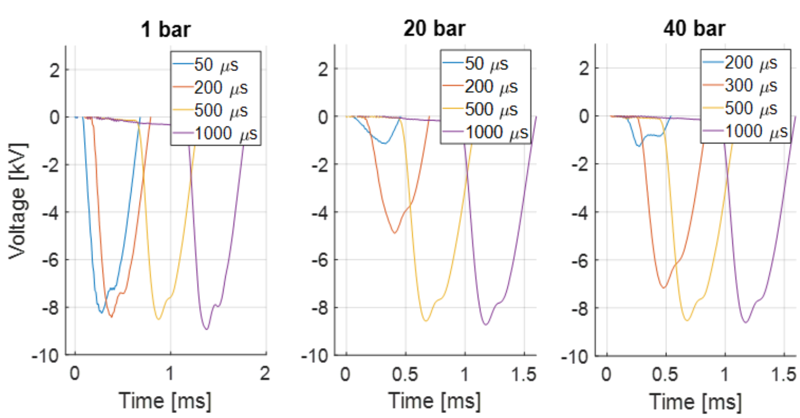

Figure 11. Change in the amplitude of the applied HV pulse at different instants after CZ in the puffer arrangement for different filling pressures.

This is the author accepted version of an article published in IEEE transactions on dielectrics and electrical insulation
http://dx.doi.org/10.1109/TDEI.2020.008844

contact gap. Due to the high mobility of electrons followed by a general drift of the charge in the gap in response to the applied voltage, the formation of the space charge layer adjacent to the electrodes is instantaneous. As a result immediately after CZ at 1 bar pressure, the breakdown voltage is close to the glow cathode-fall voltage [22]. Although no experimental data is found for glow cathode-fall voltage at a high filling pressure, an increase in the cathode-fall voltage is observed as the pressure is reduced [23].

For high filling pressures, the breakdown voltage until 300 μs is observed to be lower than at 1 bar. The energy deposition in the arc channel increases with the filling pressure due to high arc voltage. As the filling pressure is increased, the arc radius decreases [24]. Without forced gas flow, the thermal energy stored in the arc core fails to dissipate quickly. As a result, a relatively high post-arc current is observed for the arc burning at a high N_2 filling pressure [14]. A relatively high post-arc current may facilitate the glow to arc transition at high N_2 pressure, which would reduce the cathode-fall voltage [25]. In a recent study on the thermal interruption performance in the free-burning arc, the re-ignition voltage was observed to be lower at high filling pressures compared to at 1 bar [14]. In this paper, within the first 300 μs after CZ, the breakdown voltage is observed to be almost fixed. Such a plateau in the breakdown voltage with time just after CZ was also observed previously [22]. Another observation is that the duration of the plateau in the breakdown voltage is almost independent of the filling pressure.

For the free-burning arrangement, as the filling pressure increases, the breakdown voltage increases at a faster rate (after the critical time of approximately 300 μs after CZ). This critical time is probably linked with the temperature of the gap being close to the ionization temperature of N_2. Once the temperature of the gap falls below a certain level, the breakdown voltage will increase rapidly with the increase of the filling pressure, which is also observed in this paper. This fast increase in the breakdown voltage at higher pressures is also reported elsewhere [10].

The current, at least in the range investigated, has no significant effect on the dielectric recovery at any filling pressure. Perhaps the temperature of the arc core is not strongly dependent on the investigated arc currents. No strong current dependency of the arc voltage was observed during the high current phase between 150 to 450 A [12]. The inter-electrode gap, however, plays a bigger role in the recovery process. In the free-burning arc, natural convection is more efficient for a larger gap, resulting in faster arc cooling. Moreover, the breakdown voltage increases with increasing electrode gap once the temperature of the gap is below a certain level. As a result, the larger gap recovers faster and similar results are reported elsewhere for atmospheric pressure air [26].

In the free-burning arc arrangement, where natural convection is the dominant cooling mechanism after CZ, the resulting cooling of the electrode gap is not efficient. To increase the cooling of the gap, the forced convective cooling is adopted using two arrangements: a self-blast and a puffer type. As the cooling of the medium is enhanced, the recombination rate of the charge carriers after the extinction of the arc increases. The dielectric strength of the gap just after CZ is expected to be high under forced cooling. In this paper, no breakdown is observed for neither self-blast nor in the puffer setup under forced gas flow. At high pressure, however, the relatively high post-arc conductance is observed near CZ (seen as the damping of the applied HV pulse). No strong dependence of the SC state on post-arc dielectric recovery characteristics is observed. Nevertheless, forced gas flow significantly enhances the post-arc recovery at high filling pressures, also in the thermal phase. The blowing pressures for the self-blast and the puffer arrangements being different, no further comparison is made between the two blowing mechanisms.

5 CONCLUSIONS

The pressure dependence of the post-arc dielectric recovery characteristics is reported in this paper. To evaluate the recovery characteristics, an HV pulse is applied at different instants after CZ. The breakdown or hold voltage of the contact gap is analyzed as a function of time after CZ. First, the free-burning arc is investigated without forced gas flow. In the free-burning arrangement, the gap dependency and the current dependency is also studied. For the gap dependence of the recovery characteristics, a 20 and a 50 mm gap are compared for the arc current of 425 A. For the current dependence, two different amplitudes of current: 275 and 425 A are studied at 50 mm inter-electrode gap. Afterward, to investigate the effect of forced gas flow on the recovery process at different filling pressures, two different arrangements are used: a self-blast and a puffer arrangement. Depending on the experimental observations, the following conclusions are drawn:

- In the free-burning arrangement, the breakdown voltage of the contact gap increases faster with the increase of the filling pressure. However, in the thermal phase (just after CZ), the breakdown voltage is low for high filling pressure. A longer gap recovers quicker than a shorter gap. No strong current dependency of the post-arc dielectric recovery has been observed in the investigated current range.
- Forced gas flow significantly enhances the post-arc recovery at a high filling pressure, also in the thermal phase. No breakdown is observed even immediately after CZ under forced gas flow conditions for the applied currents and voltage pulses.

The experiments indicate that although the thermal phase is the critical phase of the ultrahigh-pressure N_2 arc, the dielectric phase is inherently superior as the filling pressure increases even without forced gas flow. A forced gas flow, however, also improves the performance of the thermal phase, which shows its prospects as a subsea current interruption medium.

ACKNOWLEDGMENT

This work is supported by the Research Council of Norway.

REFERENCES

[1] T. Hazel, H. H. Baerd, J. J. Legeay, and J. J. Bremnes, “Taking Power Distribution Under the Sea: Design, Manufacture, and Assembly of a Subsea Electrical Distribution System,” *IEEE Ind. Appl. Mag.*, vol. 19, no. 5, pp. 58–67, Sep. 2013.

[2] A. Nordrum, “ABB Siemens Test Subsea Power Grids For Underwater Factories - IEEE Spectrum.” [Online]. Available: https://spectrum.ieee.org/energy/fossil-fuels/abb-siemens-test-subsea-

power-grids-for-underwater-factories. [Accessed: 27-Sep-2019].

[3] E. Jonsson, "Load Current Interruption in Air for Medium Voltage Ratings," PhD dissertation, Department of Electric Power Engineering, Norwegian University of Science and Technology, Norway, 2014.

[4] Z. B. Yang, S. H. R. Hosseini, T. Kiyan, S. Gnapowski, and H. Akiyama, "Post-breakdown dielectric recovery characteristics of high-pressure liquid CO_2 including supercritical phase," *IEEE Trans. Dielectr. Electr. Insul.*, vol. 21, no. 3, pp. 1089–1094, Jun. 2014.

[5] J. Zhang, "Supercritical fluids for high power switching," PhD dissertation, Department of Electrical Engineering, Eindhoven University of Technology, Netherlands, 2015.

[6] J. Zhang, A. H. Markosyan, M. Seeger, E. M. van Veldhuizen, E. J. M. van Heesch, and U. Ebert, "Numerical and Experimental Investigation of Dielectric Recovery in Supercritical N_2," *Plasma Sources Sci. Technol.*, vol. 24, no. 2, p. 025008, Feb. 2015.

[7] K. Niayesh and M. Runde, *Power Switching Components*. Springer International Publishing, 2017.

[8] K. D. Song, B. Y. Lee, and K. Y. Park, "Analysis of Thermal Recovery for SF_6 Gas-Blast Arc within Laval Nozzle," *Jpn. J. Appl. Phys.*, vol. 42, no. Part 1, No. 11, pp. 7073–7079, Nov. 2003.

[9] M. Seeger, M. Schwinne, R. Bini, N. Mahdizadeh, and T. Votteler, "Dielectric recovery in a high-voltage circuit breaker in SF_6," *J. Phys. D. Appl. Phys.*, vol. 45, no. 39, p. 395204, Oct. 2012.

[10] M. Seeger, G. Naidis, A. Steffens, H. Nordborg, and M. Claessens, "Investigation of the Dielectric Recovery in Synthetic Air in a High Voltage Circuit Breaker," *J. Phys. D. Appl. Phys.*, vol. 38, no. 11, pp. 1795–1804, Jun. 2005.

[11] T. Nakano *et al.*, "Thermal Re-ignition Processes of Switching Arcs with Various Gas-blast Using Voltage Application Highly Controlled by Powersemiconductors," *J. Phys. D. Appl. Phys.*, vol. 51, no. 21, p. 215202, May 2018.

[12] F. Abid, K. Niayesh, E. Jonsson, N. S. Stoa-Aanensen, and M. Runde, "Arc Voltage Characteristics in Ultrahigh-Pressure Nitrogen Including Supercritical Region," *IEEE Trans. Plasma Sci.*, vol. 46, no. 1, pp. 187–193, Jan. 2018.

[13] F. Abid, K. Niayesh, and N. S. Stoa-Aanensen, "Ultrahigh-Pressure Nitrogen Arcs Burning Inside Cylindrical Tubes," *IEEE Trans. Plasma Sci.*, vol. 47, no. 1, pp. 754–761, Jan. 2019.

[14] F. Abid, K. Niayesh, S. B. Thimmappa, C. Espedal, and N. Støa-Aanensen, "Thermal Interruption Performance of Ultrahigh-Pressure Free-Burning Nitrogen Arc," in *21st International Symposium on High Voltage Engineering (ISH)*, Berlin, Heidelberg: SPRINGER, 2020, pp. 663–671.

[15] F. Abid, K. Niayesh, and N. Støa-Aanensen, "Nozzle Wear And Pressure Rise In Heating Volume of Self-Blast Type Ultra-High Pressure Nitrogen Arc," *Plasma Phys. Technol. J.*, vol. 6, no. 1, pp. 23–26, 2019.

[16] F. Abid, K. Niayesh, and N. Støa-Aanensen, "Arc Voltage Distribution Measurement in Tube Constricted Ultrahigh-Pressure Nitrogen Arc," in *International Symposium on High Voltage Engineering (ISH)*, Budapest, Hungary: Springer Nature, 2020, pp. 672–679.

[17] F. Abid, K. Niayesh, and N. Stoa-Aanensen, "Post-arc Dielectric Recovery Characteristics of Free-burning Ultrahigh-Pressure Nitrogen Arc," in *2019 5th International Conference on Electric Power Equipment - Switching Technology (ICEPE-ST)*, 2019, pp. 105–108.

[18] A. Kadivar and K. Niayesh, "Two-way interaction between switching arc and solid surfaces: distribution of ablated contact and nozzle materials," *J. Phys. D. Appl. Phys.*, vol. 52, no. 40, p. 404003, Oct. 2019.

[19] H. Edels, D. Whittaker, K. G. Evans, and A. B. Shaw, "Experiments and Theory on Arc Reignition by Spark Breakdown," *Proc. Inst. Electr. Eng.*, vol. 112, no. 12, p. 2343, 1965.

[20] G. Farrall and J. Cobine, "Recovery Strength Measurements in Arcs from Atmospheric Pressure to Vacuum," *IEEE Trans. Power Appar. Syst.*, vol. PAS-86, no. 8, pp. 927–932, Aug. 1967.

[21] H. Edels and J. C. Holme, "Measurements of the Decay of Arc Column Temperature Following Interruption," *Br. J. Appl. Phys.*, vol. 17, no. 12, pp. 1595–1606, Dec. 1966.

[22] F. W. Crawford and H. Edels, "The Reignition Voltage Characteristics of Freely Recovering Arcs," *Proc. IEE Part A Power Eng.*, vol. 107, no. 32, p. 202, 1960.

[23] J. P. Novak, "Electric field and electrode potential drops of arcs and glow discharges in air," *J. Appl. Phys.*, vol. 62, no. 12, pp. 4719–4724, Dec. 1987.

[24] T. OKUMA *et al.*, "Effects of Working Pressure on Temperature Characteristics in Multiphase AC Arc," *J. Fluid Sci. Technol.*, vol. 13, no. 4, pp. JFST0024–JFST0024, 2018.

[25] W. A. Gambling and H. Edels, "The high-pressure glow discharge in air," *Br. J. Appl. Phys.*, vol. 5, no. 1, pp. 36–39, Jan. 1954.

[26] A. B. Shaw and D. Whittaker, "Effect of Gas Flow on Post-Arc Gap Recovery," *Proc. Inst. Electr. Eng.*, vol. 111, no. 1, p. 193, 1964.

Fahim Abid was born in Jamalpur, Bangladesh in 1990. He completed the B.Sc. degree in Electrical and Electronic Engineering in 2012 from the Islamic University of Technology (IUT), Bangladesh. He received the M.Sc. degree in 2015 on Electrical Engineering from the Royal Institute of Technology (KTH), Sweden. He is currently working on his Ph.D. degree at the Department of Electric Power Engineering at Norwegian University of Science and Technology (NTNU), Norway.

Kaveh Niayesh (S'98–M'01–SM'08) completed the B.Sc. and M.Sc. degree in Electrical Engineering from the University of Tehran, Iran, in 1993 and 1996 respectively. In 2001, he completed the Ph.D. degree from the RWTH-Aachen University of Technology in Electrical Engineering. In the last 19 years, he held different academic and industrial positions including Principal Scientist with the ABB Corporate Research Center, Baden-Dattwil, Switzerland; Associate Professor with the University of Tehran; and Manager, Basic Research, with AREVA T&D, Regensburg, Germany. Currently, he is a Professor in the Department of Electric Power Engineering at Norwegian University of Science and Technology (NTNU), Norway. He is the holder of 16 patents and has more than 120 journal and conference publications on current interruption and limitation, vacuum and gaseous discharges, plasma modeling and diagnostics, and pulsed power technology.

Egil Viken is currently working with his M.Sc. in electrical power engineering from the Norwegian University of Science and Technology (NTNU), Trondheim, Norway. He is in the final year of his master and is planning to graduate summer 2020. He worked in SINTEF with current interruption as an intern the summer 2018 and 2019.

Nina Sasaki Støa-Aanensen completed the M.Sc. degree in Applied Physics and Mathematics in 2011 and the Ph.D. degree in Electrical Power Engineering in 2015 from the Norwegian University of Science and Technology (NTNU), Trondheim, Norway. Currently, she is working as a research scientist in SINTEF Energy Research, Trondheim, Norway.

Erik Jonsson received the M.Sc. degree in physics in 2005 from Uppsala University, Sweden. He completed the Ph.D. degree in Electrical Power Engineering in 2014 from Norwegian University of Science and Technology (NTNU), Trondheim, Norway. He worked with ABB Corporate Research, Västerås, Sweden from 2006 to 2007. Currently, he is working as a research scientist in SINTEF Energy Research, Trondheim, Norway.

Hans Kristian Meyer completed his M.Sc. degree in 2015 and Ph.D. degree in 2019 on Electric Power Engineering from the Norwegian University of Science and Technology (NTNU) in Trondheim, Norway. Currently he is working as a research scientist in SINTEF Energy Research, Trondheim, Norway.

This is the author accepted version of an article published in IEEE transactions on dielectrics and electrical insulation
http://dx.doi.org/10.1109/TDEI.2020.008844